IEEE Access
Multidisciplinary | Rapid Review | Open Access Journal

Received September 18, 2020, accepted September 22, 2020, date of publication September 28, 2020,
date of current version October 8, 2020.

Digital Object Identifier 10.1109/ACCESS.2020.3027033

Coplanar Waveguide Based Sensor Using Paper Superstrate for Non-Invasive Sweat Monitoring

MICHAEL M. Y. R. RIAD AND A. R. ELDAMAK, (Member, IEEE)
Department of Electronics and Electrical Communication Engineering, Faculty of Engineering, Ain Shams University, Cairo 11517, Egypt
Corresponding author: Michael M. Y. R. Riad (michael.riad@eng.asu.edu.eg)

ABSTRACT This paper presents a broadband, simple, re-useable and low-cost approach for noninvasive sweat monitoring using a passive microwave circuit and a cellulose filter paper as a superstrate. The proposed sensor is composed of filter paper with the ability to absorb the sample liquid under test (LUT) placed on top of a coplanar waveguide (CPW) transmission line. Various samples of sodium chloride (NaCl) solutions with concentrations in the range of 0.01-2 mol/L and models of artificial sweat are used to test the proposed sensor. The difference in transmission coefficient (S_{21}) between dry and wet states is used to determine the concentrations of tested solutions in the band of 1-6 GHz. The sensor detects concentrations as low as 0.01 mol/L (0.58 g/L) and quantities as low as 137 μL with a maximum sensitivity of 46.7 dB/g/L. The proposed sensor presents a simple approach to sample and characterize liquids with enhanced sensitivity and consistent performance using microwave signals.

INDEX TERMS Microwave bio-sensing, paper superstrate, hydration sensor, cystic fibrosis diagnosis, liquid characterization, re-useable sensor, sweat monitoring.

I. INTRODUCTION

With the increasing interest in early diagnosis and therapeutic technologies, there is a growing interest in analyzing biofluids. Biofluids including urine, blood, tears and sweat carry physiological biomarkers that can reflect health status. Normally, blood carries highly accurate information on the human body. With a composition of sweat that is osmotically related to blood, sweat is an excellent candidate for easy, fast and non-invasive monitoring. This will allow the diagnosis of diseases such as Cystic fibrosis (CF) and dehydration via sweat monitoring.

Cystic fibrosis (CF) is a genetic disorder disease that affects the production of mucus in the respiratory, digestive and reproduction systems and causes fatal lung infections [1]. In the United States and the United Kingdom, the average life expectancy for a CF patient is 35 to 40 years old whereas in countries such as India, El Salvador, and Bulgaria, the life expectancy drops to below 15 years [2]. The standard test for CF is a sweat test. Patients with CF have excess salt (NaCl) in their sweat with concentrations of 60 mmol/L or higher [3].

The associate editor coordinating the review of this manuscript and approving it for publication was Farid Boussaid.

However, CF is not the only medical condition that may contribute to an increased concentration of NaCl in sweat. Dehydration can also contribute to an increased concentration of NaCl in the sweat. Dehydration occurs when the body losses a large amount of water without replacement [4]. The most common reasons for dehydration are vigorous exercise, diarrhea, vomiting, fever, and hot weather [4]. In addition to affecting the cognitive and physical abilities, dehydration can increase the likelihood of developing deep vein thrombus (DVT) and pulmonary embolism (PE) which has a high morbidity rate if not caught early [5]–[7]. In the U.S., It is estimated that 100,000 people die each year due to PE [7]. This is caused by a mobile DVT going into the lungs, and 25% of those who are affected by a PE die without a warning [7]. COVID-19 has been linked to an increased risk of thrombosis [8], [9]. Moreover, the accompanying lock down, has decreased the activity of individuals significantly and thus, there is a much higher risk to develop DVTs [5]–[7].

Human sweat is mainly composed of sodium, chloride, potassium, magnesium, zinc, iron, calcium, copper phosphate, uric acid, urea, lactic acid as well as amino acids [10]. Among major sweat components, tracking sodium (Na+), chloride (Cl-) and potassium (K+) can provide information

on the water-salt balance in human tissues, hydration levels, and the presence of cystic fibrosis [3].

Moreover, sweat collection does not require needles or induce pain which makes it suitable even for infants who are just a few days old [3]. The cystic fibrosis foundation had issued some guidelines [3] for a well-performed and interpreted sweat test. Those guidelines include recommended collection methods, inducing the sweat by pilocarpine iontophoresis, the amount of sweat sample which should be at least 75 mL and the lower limit of detection should be at least 10 mmol/L for NaCl concentration. For a positive test, the sweat chloride concentration should be at least 60 mmol/L for several consecutive tests [3]. Generally, the concentration of sodium ions (Na+) varies from 20-70 mmol/L [11] in healthy individuals, although it can be affected by other factors such as fitness level and acclimation.

Several sensors have been reported in literature that monitor electrolytes in sweat [11]–[13]. This includes using skin potentiometric sensors [11], impedimetric sensors [12], and multi-biomarker selective patches [13]. However, these devices require continuous contact with the skin during measurements. This increases the complexity of sensing and requires extensive testing to understand the effect of other variables related to skin tissues such as age and gender.

Recently microwave-based sensors offer a non-invasive solution to characterize biofluids [14]–[24]. Body fluids with different electrolytic concentrations can result in different losses and hence attenuation of electromagnetic waves. The detected reflected or transmitted signals carry information on electrolytic concentrations, motivating the development of non-invasive microwave-based sensors. This includes tracking concentrations of NaCl [14], [15], [21]–[23], glucose [16]–[21], KCl and CaCl [22]. The distinctive dielectric properties of biofluids could help in monitoring kidneys status through urine [22], diabetes through glucose levels [17]–[20], [25], [26], dehydration through sweat [23], [24], [27] and blood [28]. Among different sensors reported for tracking electrolytes [11]–[27], sodium chloride (NaCl) results in the largest recorded variations with changing hydration states [23], [24].

In [23], our group presented a resonator-based conformal and disposable sensor to track the concentrations of NaCl in sweat in the band of 2-4 GHz. The sensor is composed of a microstrip patch antenna with filter paper acting as substrate. The filter paper is meant to absorb the liquid under test (sweat). Using reflection-based measurements, NaCl concentrations in the range of 8.5–200 mmol/L, representing different hydration states are detected. On the other side, reflection-based sensors provide narrow-band sensing and they are less feasible than transmission-based sensors in integration with real world applications. For such systems, it is necessary to use Vector Network Analyzer (VNA) to separate and measure the incident and the reflected waves.

In this paper, a broadband transmission-based non-invasive, and low-cost sensor to track NaCl concentration in sweat is presented. This work aims to elevate the concept of using filter papers as a substrate for a microwave-based sensor presented in [23]. Instead of disposing both paper substrate and microwave circuit in [23], only the filter paper used as a superstrate to a CPW line will be disposed after each sample. The proposed sensor will be re-useable instead of being disposable with more structural integrity and an overall lower cost. The proposed sensor is transmission-based with minimal requirements for complementing devices. The filter paper is meant to sample the liquid under test (sweat) and the changes in the electrolytes concentrations is inferred from the transmission levels.

The rest of the paper is organized as follows, section II explains the design of the sensor, section III explains the sensing approach in terms of the interface technique, section IV explains the experimental measurement procedures including sample preparation, section V showcases the simulation and measurement results, section VI discusses the results by comparing it to similar work in literature and finally the work is concluded in section VII.

II. SENSOR DESIGN

CPW lines have demonstrated higher sensitivity in dielectric properties extraction and material characterization compared to microstrip and slot lines [12], [18], [22], [24], [29]–[32]. Normally, microstrip-based structures are used in resonance-based sensors due to the sensitivity of the microstrip gap. On the other side, CPW modes are associated with fringing fields that are less confined in the substrate compared to microstrips. Although slot-lines also acquire fringing fields as CPW, they are not compatible with a standard SMA connector and the radiation losses might impact the sensing results. Therefore, slot-lines may not be suitable for direct transmission-based sensors as CPWs.

CPWs have been used as material sensors in the literature [33]–[37]. In [33]–[36], a resonator itched on the central conductor was used to detect wetness [33], and characterize liquids such as oils [34], [36], and biological samples [35]. Moreover, CPWs are frequently used in different circuits including filters, couplers and power dividers which can be adapted into high sensitivity sensors. In [37], 4 CPW lines used as input ports for a directional coupler were used to measure the complex permittivity of a solid sample.

In the proposed sensor, the CPW line is implemented on FR4 substrate with dielectric constant ε_r of 4.4, losses ($tan\ \delta$) of 0.02 and height h of 1.6 mm. The substrate has width (wt) of 40 mm, and length L of 50 mm. The dimensions of the CPW line shown in Fig.1 are strip width (ws) of 2 mm, gap width (g) of 2 mm and conductor thickness t of 50 μm. These dimensions correspond to a characteristic impedance of 100 Ω. This impedance was chosen to increase the size of the gap width to 2 mm compared to 0.3 mm for 50 Ω line. The chosen line impedance of 100 Ω is a tradeoff between fabrication tolerance, acquiring sturdy soldering and low insertion loss of −2.13 dB across the operating band (illustrated in Fig.3).

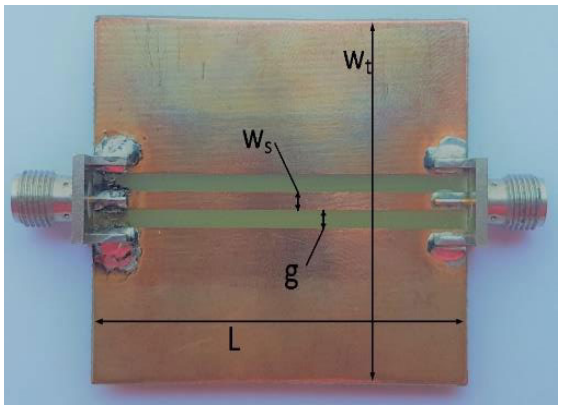

FIGURE 1. Top view of the manufactured CPW-based sensor.

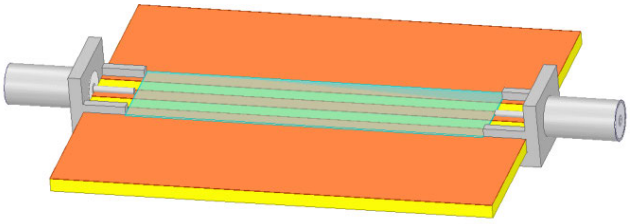

FIGURE 2. Simulation model of CPW-based sensor showing the CPW line, the two connectors and the layer representing paper superstrate or liquid under test (shown in green).

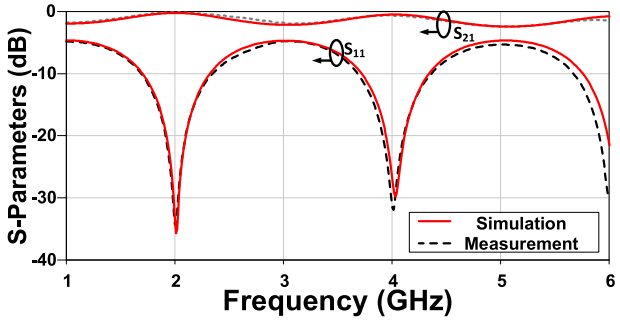

FIGURE 3. Measured and simulated S-parameters of the CPW-based sensor versus frequency without paper superstrate.

The CPW transmission line is simulated using HFSSv15.0 in the range of 1-6 GHz. The simulation model is shown in Fig. 2. It is composed of the CPW line and the two connectors inside an air box with radiation boundary. A layer of height 180 μm (shown in green in Fig.2) represents the filter paper and is placed on top of the CPW line. The dielectric properties of this layer will be equivalent to tested saline solutions with NaCl concentrations in the range of 0.01-2 mol/L. The excitation port is placed at the end of the SMA connectors from which S-parameters are recorded. Thus, the simulations mimic real prototype with connectors added to the sensor model.

The sensor was fabricated and measured using Anritsu (MS4647A) Vector Network Analyzer (VNA). Fig 3 shows the measured and simulated reflection coefficient (S_{11}) and transmission coefficient (S_{21}) of the structure. The measurements were in good agreement with simulation with three transmission ($|S_{21}|$) peaks of 0 dB at 2, 4, and 6 GHz.

III. SENSING APPROACH

The key idea in the proposed sensing approach is to place the filter paper on top of the CPW line. The paper will be used to sample the intended liquid under test (LUT) using a pipette, or through direct absorption from a surface such as the skin for sweat collection. The paper superstrate is Whatman Grade 1 (WHA1001090) filter paper and has a thickness of 180 μm. The dielectric properties of the paper were characterized previously by our group in [23] with dielectric constant ε_r of 1.9, and losses (tan δ) of 0.025.

Different approaches for sample placement were reported in literature in [14], [18]–[22], [31], [34], [36], [38]–[41]. These approaches include using containers either placed on the sensor [20], [34]–[36], [40] or in proximity to the sensor [38]. Although the container approach allows using big sample size, it usually wastes a large portion of the sensitive surface of the sensor due to the thick walls of the containers. Moreover, most of this volume was added in the vertical direction away from the circuit where the fringing fields are almost absent. Thus, the sensitivity is not improved as most of the liquid is not sampled by the field. In [40], A method to increase the sampled volume by adding two aluminum blocks on top of a resonator was proposed. However, this is not applicable to most sensor designs. Other approaches such as fluidic channels [14], [19], [21], [22], [39], and capillary tubes [18], [31], [41] also exist. However, a major drawback with capillary tubes and fluidic channels is that they usually require extra amount of liquid to ensure that the capillary or channel is full where it gets in contact with the sensor. Moreover, the cylindrical shape of capillaries limits its contactability to the flat surface of the circuit. Those approaches also require complementary mechanical systems such as pumps or syringes to fill or empty the liquid. These mechanical systems will contribute to the cost of the final system.

Another reported approach is to apply drops of the liquid directly on top of the circuit [30], [33]. However, this technique requires precision in the exact location on which the drops land. This is because any error in the location of the drops will contribute to the instability of the results. Moreover, those techniques are unpractical for sampling and collection of some biofluids such as sweat which usually limited in quantity.

In the proposed sensor, the filter paper damped with intended LUT is placed on the sensor. Being in full contact with the sensing surface and the homogenous distribution of the sample is expected to boost the sensitivity of the proposed sensor. The LUT will alter the electrical properties of paper superstrate. Thus, the fringing fields of the CPW line will interact with new dielectric properties and consequently, differences in measurements for transmission coefficients (S_{21}) will occur. The differences between dry and

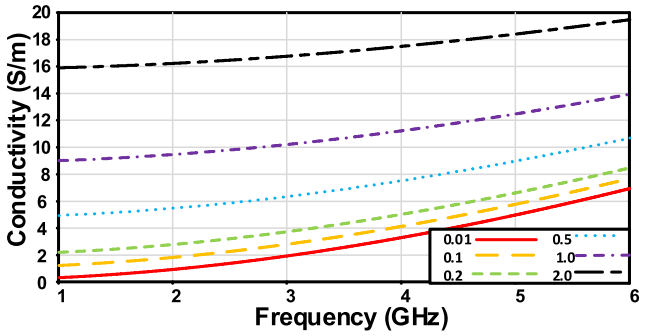

FIGURE 4. Calculated conductivity versus frequency for NaCl solutions at concentrations 0.01-2 mol/L used in simulations.

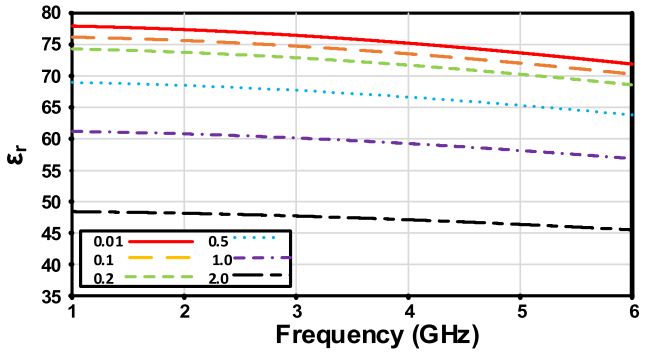

FIGURE 5. Calculated relative permittivity versus frequency for NaCl solutions at concentrations 0.01-2 mol/L used in simulations.

wet states should provide an indication about the electrical properties of the LUT. This could be used to generally characterize liquids and track concentrations of different biofluids. Specifically, with the proposed approach, electrolytes in sweat could be monitored. This could help in diagnosis of dehydration and CF through sweat. Among major sweat electrolytes [14], [23], [24], NaCl has been proved to have the dominant effect in changing electrical properties of sweat over the other components [23], [24].

In order to validate the operation of the proposed approach, the sensor will be tested with solutions of different concentrations of NaCl in both simulations and measurements. The set of concentrations used in simulations were in the range 0.01-2 mol/L. These values match concentration of the samples prepared for measurements and representing different hydration states. Usually, the concentrations of NaCl in sweat for normal and dehydration states are 0.01 and 0.1 mol/L respectively [23], [24]. Moreover, a concentration higher than 0.06 mol/L is an indication that cystic fibrosis is a likely diagnosis [3].

The expected range for the measurements is much smaller than our proposed range. Yet, it was necessary to explore larger dynamic range of the sensor in order to avoid misleading results at higher concentrations. Furthermore, it can indicate whether the sensor is viable with other biofluids such as urine, or other industrial applications with higher concentrations of NaCl.

TABLE 1. Measured dielectric properties of distilled water (DW), and different NaCl Solutions at 2 GHz.

Material	ε_r	tan δ	σ(S/m)
Distilled Water	77.49	0.0971	0.846
NaCl (0.01 mol/L)	77.725	0.1176	1.027
NaCl (0.10 mol/L)	76.882	0.2081	1.8
NaCl (0.20 mol/L)	75.855	0.3435	2.93
NaCl (0.35 mol/L)	74.655	0.5052	4.236
NaCl (1.00 mol/L)	66.107	1.2971	9.63
NaCl (1.70 mol/L)	52.288	2.4247	14.51

The CPW line is simulated with a layer of thickness 180 μm on top of it. This thickness is equivalent to the paper superstrate that will be placed in the experiment. The electrical properties of this layer will be equivalent to the intended liquid under test. The calculated conductivity and relative permittivity of the NaCl solutions versus frequency are shown in Fig.4, and Fig.5 respectively. These properties were obtained using the equations described in [42], calculated using GNU Octave v5.1.0 for each individual concentration and imported into HFSSv15.0 for simulation. Table 1 shows the permittivity and conductivity of distilled water (DW) and different saline solutions at 2 GHz (frequency of interest). The given properties in Table 1 were measured experimentally by our group using a dielectric probe (87050E, Keysight Technologies) and reported in [24]. These measured values are within 2-5% from the calculated values shown in Fig.4 and Fig.5. All materials used in the proposed sensing system including Air ($\varepsilon_r = 1$, $\tan\delta = 0$), FR4 (substrate of sensor), Pure DW and NaCl solutions do not acquire magnetic properties. Thus, they all have relative permeability μ_r of 1. The results of the simulations are presented and compared to measurements in section V.

IV. TEST SOLUTIONS & EXPERIMENTAL SET UP

In order to start measurements, six samples of NaCl solutions with concentrations 0.01, 0.1, 0.2, 0.5, 1, and 2 mol/L were prepared. These concentrations are similar to those used in simulations. The preparation process was as following: A commercial grade table salt was weighted using a scale of 0.0001 grams precision. 1 mol of NaCl is equivalent to 58.44 grams. Therefore, 0.5844, 5.844, 11.688, 29.22, 58.44 and 116.88 grams were prepared and stored separately in an air-tight container to avoid any exposure to moisture. On the day of measurement, the salt samples were each added to 1 liter of Distilled Water (DW) in a clean glass graded cylinder. Then it was stirred rigorously using a clean glass stirring rod till no trace of solid salt crystal was visible.

The samples were then placed inside clean sealed cups to prevent evaporation. The cups were medical grade disposable collection cups which grantees that no reaction to saline solutions would take place. The samples were then left to rest for at least an hour in a temperature-controlled environment to remove any air that might have been trapped during the preparation process. This makes sure that all the solutions have reached an equilibrium ambient temperature. In order

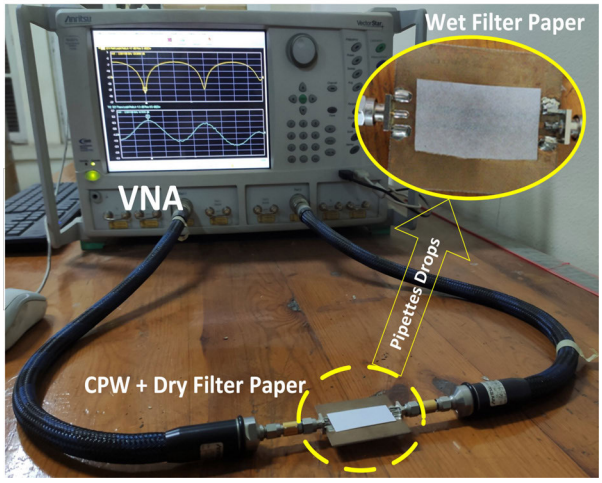

FIGURE 6. Measurement setup showing the Vector Network Analyzer (VNA) connected to the CPW-based sensor loaded by a dry filter paper. Inset figure shows zoom-in for a wet filter paper after applying drops of LUT using pipette.

to apply the LUT samples on the filter paper, disposable pipettes were used. All from the same batch, the drop weight is calibrated through 60 rounds of measurements using a high precision scale. The average volume of one drop from the calibrated pipette is 34.4 μL.

The measurement setup used with the proposed sensor is shown in Fig.6. It is composed of the CPW transmission line and paper superstrate connected to the VNA. Fig.6 shows a zoom in for filter paper cut using scissors into a rectangular shape of size 40 mm x18 mm and after applying LUT using pipette. This length is equal to the whole length of the transmission line ($\lambda/2$ at 2 GHz) till the edges of the two SMA connectors. The width of the paper superstrate covers both gaps of the CPW where most of the field exists.

The measured S-Parameters were acquired using Anritsu MS4647A vector network analyzer (VNA) with measurement range up to 70 GHz. Both ports of the VNA were calibrated before each measurement session. The calibrated range was from 1 GHz to 6 GHz with 1001 points per sweep. The measurements are divided into two categories; dry and wet measurements. The dry measurements include the unloaded CPW, the CPW loaded by dry filter paper, and the CPW which has been wiped dry by lint free wipes after each measurement. The purpose of the dry measurements is to investigate whether there is a loading effect from the filter paper and whether the sensor would have a memory effect from previous measurements. The results of the dry measurements are shown in Fig. 7. It is apparent that the dry filter paper has a minimal loading effect on the CPW's response. Moreover, the CPW-based sensor retains its response when dried post measurement with LUT as shown in Fig.7. Thus, the sensor is reusable and retains its response post measurement.

The wet measurements are conducted using the CPW line and paper superstrate damped with the saline solutions. Wet measurements with saline solutions were divided into three

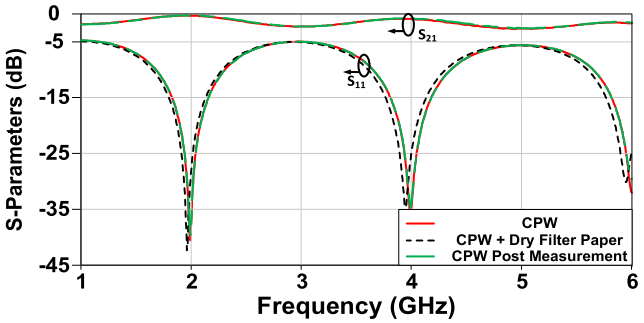

FIGURE 7. S-parameters versus frequency for the unloaded CPW, the CPW loaded with dry filter paper, and the CPW wiped out dry post measurement.

separate rounds. The rounds were at least one day apart. This was intended to investigate the effect of day to day unintentional variations such as temperature, filter paper size, filter paper positioning, the exact quantity of the solution, cable connections, and VNA calibration on the accuracy of measurements and detection. In each round, each concentration was measured six times at two different liquid quantities (4 drops and 6 drops). For each quantity, three rounds of measurements were recorded. First, a quantity of 4 drops (137 μL) is added to the paper superstrate. This is followed by adding another 2 drops, so the total amount of liquid under test is 6 drops (206 μL). The results of three measurement rounds were averaged and compared in section V. The effect of changing the quantity and concentration of LUT on the measurements will be also discussed. The total quantity of the solution absorbed by filter paper is 6 drops corresponding to 206 μL. Although this quantity of sweat is significantly lower than the recommendation of the CFF (75 mL) [3], it should provide sufficient accuracy due to the high sensitivity of the proposed sensing approach.

During measurements, accidental air gaps could form when applying the wet filter paper to the flat surface of CPW line as shown in Fig.8(a). These air gaps can contribute to a significant error up to 15% in the measured values of S_{21}. Therefore, any visible air gaps should be removed by tapping the filter paper with a smooth rounded object to avoid tearing the paper. Fig.8(a) shows an air gap after applying LUT while Fig.8(b) shows the same filter paper after the air gap was removed using the smooth backside of the pipette. Once the air gap is removed, measurement error is eliminated.

V. RESULTS

Starting from almost 0 dB transmission, increasing the NaCl concentration increases conductivity and consequently losses. Fig. 9(a) shows the simulated transmission (S_{21}) while Fig. 9(b), 9(c) show the measured S_{21} for 4 and 6 drops respectively at different concentrations. In order to explain the recorded data, a comparison is performed at a single frequency of 2 GHz. This corresponds to the first half wavelength resonance of the original structure with reference level of almost 0 dB. Table 2 summaries the transmission values at 2 GHz for the EM simulations as well as the measurements of 4 and 6 drops for each concentration.

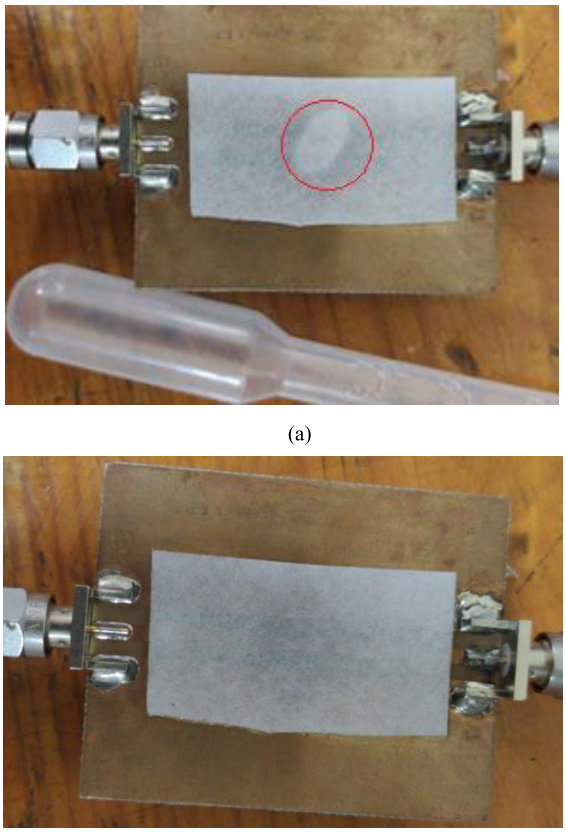

FIGURE 8. Top view of the CPW line with the wet filter paper (a) with an air gap (inside the red circle). (b) after the air gap was removed using the smooth back side of the pipette.

TABLE 2. Simulated and Measured Transmission results at 2 GHz.

Concentration (Mol/L)	S_{21}(dB) for Simulations	S_{21}(dB) for 4 Drops	S_{21}(dB) for 6 Drops
0.01	-2	-2.51	-3.925
0.1	-3.63	-4.35	-5.951
0.2	-5.41	-5.93	-8.046
0.5	-10.24	-10.14	-13.231
1	-17.25	-15.6	-20.158
2	-27.67	-22.67	-28.494

From Table 2, the simulation results show similar behavior to the measurements. However, it was lower than the 4 drops in the 0.01-0.2 mol/L range, whereas it became higher than 4 drops in the 0.5-2 mol/L range. On the other hand, the measurements of the 6 drops quantity remained significantly higher than simulation across the whole range of samples.

Since the sensor would be used in a biomedical application, it is essential to investigate some measurement uncertainties that can affect the results. One of which is the location where the drops are applied. Although the filter paper would absorb the LUT and distribute it across the sensor's surface, there is no guarantee that the distribution is completely homogenous. In order to investigate this effect, the drops of a saline solution with NaCl concentration of 0.1 mol/L are applied to the filter paper at three different positions; the center (nominal case),

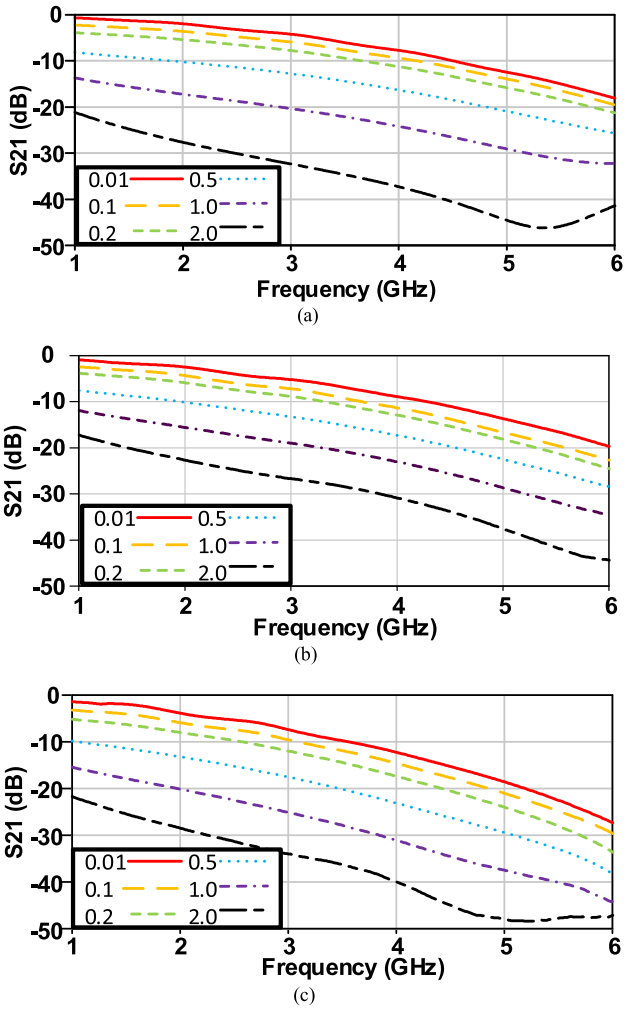

FIGURE 9. S_{21} (dB) versus frequency for CPW based sensor loaded with filter paper sampling NaCl solution with concentrations in the range of 0.01-2 mol/L (a) simulations, (b) 4 drops measurements, (c) 6 drops measurements.

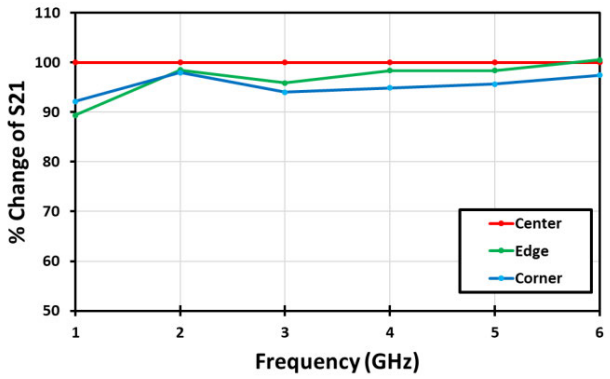

FIGURE 10. Percentage of change in magnitude of S_{21} versus frequency at different positions of dropping LUT to the filter paper. The values are normalized to the nominal case of dropping LUT at the center of the filter paper and shown as a 100% line.

the corner and the edge. The experiment was repeated 3 times and variations in magnitude of S_{21} due to changing position of

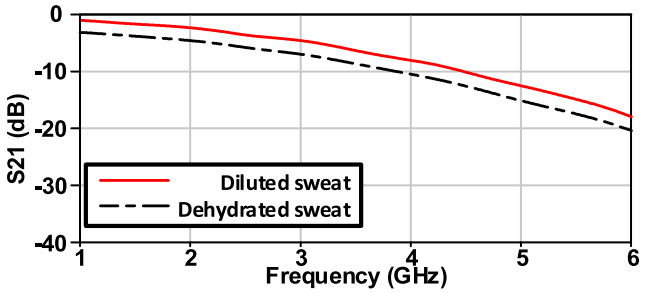

FIGURE 11. Simulated S_{21} (dB) versus frequency for CPW-based sensor using models for artificial sweat representing dehydrated and diluted (normal) states.

dropping LUT are recorded and averaged. Fig. 10 shows the percentage of change in S_{21} at different locations compared to the nominal case at center. From Fig. 10, position of the drops can introduce variations of 2-6% to magnitude of S_{21} across the band of 2-6 GHz.

To further validate the operation of the proposed sensor to monitor sweat, the electrical properties of artificial sweat characterized in [24] representing normal and dehydrated states will be used in simulations. Artificial sweat recipe in [24] follow the European standard (EN1811:2011) presented in [23], [24]. The electrical properties were measured using a dielectric probe (87050E, Keysight Technologies) and imported to EM simulator HFSSv15.0. Using the measured dielectric properties, simulation results with samples of dehydrated (DHS) and diluted (DS) are shown in Fig. 11. At 2 GHz, the diluted sweat had a transmission coefficient (S_{21}) of -2.37 dB and for dehydrated sweat, the transmission coefficient was -4.61 dB. As expected, the results for the diluted sweat was slightly higher than the 0.01 mol/L concentration of NaCl. Moreover, the dehydrated sweat had a result in the range 0.1-0.2 mol/L. This could be attributed to differences in dielectric constant and conductivity of solution composed of solely NaCl and artificial sweat with other components (KCl, Urea and Lactic acid).

VI. DISCUSSION

This work proposes a simple, low cost and reusable microwave-based sensor for hydration monitoring and cystic fibrosis diagnosis. The proposed sensor is composed of a standard structure of a CPW line with a filter paper as a superstrate. Various simulations and experiments had been conducted with solutions of NaCl with concentrations in the range of 0.01-2 mol/L and with quantities of 134-206 μL. Moreover, the sensor is tested with models of artificial sweat representing normal and dehydrated states.

The proposed sensor demonstrates the ability to track electrolytes with different concentration across broad bandwidth in the range of 1-6 GHz. The proposed sensor successfully detected concentrations of NaCl solutions as low as 0.01 mol/L (0.58 g/L) through transmission measurements (S_{21}). Also, it successfully differentiates normal and dehydrated states at 0.01 mol/L and 0.1 mol/L respectively with difference of 2.24 dB. This proves the feasibility of the proposed structure, and interface technique.

TABLE 3. Comparison with other Electrolyte Microwave sensors.

Ref.	Max. sensitivity (dB/g/L)	Resolution (g/L)	Dynamic range (g/L)
[16], Glucose	0.003	1	300
[17], Glucose	1.75	1.5	5.5
[18], Glucose	0.017	10	150
[19], Glucose	0.003	5	300
[20], Glucose	1.56	0.5	2.5
[21], Glucose	0.055	1	100
[14], NaCl (0.9 GHz)	4.3	0.25	80
[15], NaCl (4.0 GHz)	0.005	2	10
[21], NaCl (0.7 GHz)	1.609	0.5	100
[22], NaCl (0.9 GHz)	12.27	0.25	60
This work (2.0 GHz)	**6.716**	**0.58**	**116**
This work (6.0 GHz)	**46.71**	**0.58**	**116**

A quantitative comparison with other microwave-based sensors tracking electrolytes in literature is presented in Table 3. The figures of merit shown in Table 3 including resolution, maximum sensitivity, and dynamic range are used to evaluate performance of sensors in [21], [22]. The resolution is defined as the minimum concentration a sensor was able to detect. In our case, the least concentration tested was 0.01 mol/L which corresponds to 0.5844 g/L. This represents concentration of NaCl in diluted or normal sweat for sweat monitoring applications. Concentrations below 0.01 mol/L were not investigated as it is not relevant to targeted applications for sweat monitoring.

The sensitivity is defined as the change in dB from the reference level divided by the corresponding concentration. In our case, the reference level was 0 dB, and the magnitude of S_{21} at 2 GHz was 3.925 dB at 0.5844 g/L. This corresponds to sensitivity of 6.716 dB/g/L (maximum sensitivity at 2 GHz across the range of concentrations). In terms of quantity of LUT, the sensitivity of the 4 drops quantity (max. 4.295 dB/g/L) is lower than the sensitivity of the 6 drops (max. 6.716 dB/g/L).

Finally, the dynamic range is defined as the maximum tested and detectable concentration. In our case, the maximum tested concentration was 2 mol/L (116.88 g/L). In this work it was decided to stop testing at 2 mol/L as the highest concentration. This corresponds to 116 g/L which is beyond any concentration that is physiologically possible in sweat.

The proposed sensing approach acquire the highest sensitivity except for the work in [22]. Despite its higher sensitivity, the sensor in [22] has a reduced dynamic range of 60 g/L compared to 116 g/L in this work. Also, the sensor in [22] is insensitive to increasing concentration beyond 60 g/L at 0.9 GHz. Moreover, by increasing the operating frequency of the proposed sensor to 6 GHz, a significant boost in sensitivity to 46.71 dB/g/L could be realized. The increased sensitivity at 6 GHz, can be explained by the significant increase in the conductivity for all the investigated concentrations as shown in Fig.4. The sensor could resolve concentration

of 1 mol/L and 2 mol/L with a difference of 3 dB at 6 GHz compared to 8.5 dB at 2 GHz. This makes the higher frequencies a great candidate for detecting solutions with lower concentration. Furthermore, compared to the other NaCl sensors, this work achieved the highest dynamic range at 2 GHz. Moreover, Table 3 shows that the proposed sensing technique is comparable in performance to much more complex sensing structures presented through [14]–[22]. Compared to the other NaCl sensors, this work achieved the highest dynamic range (above 100g/L) at 2 GHz.

One of the challenges in designing a sensor is the large dataset required in the calibration process in order to create a robust model of the sensor's behavior under various stimuli. This dataset requires a lot of time and effort to gather experimentally. Therefore, it is favorable to develop a model either through curve fitting [14], [22], principle component analysis (PCA) [43], [44], or machine learning [45] to predict concentrations that were not used in the creation of the model. The complexity of the method will depend on the complexity and dimensionality involved in the sensing process. Since the proposed sensor is used to characterize mainly one independent variable which is the concentration of electrolytes, simple curve fitting techniques should provide adequate accuracy. The fitting technique used was 3rd order polynomial. The concentration can be calculated from the magnitude of S_{21} in dB at 2 GHz using (1), this expression has a correlation coefficient $R^2 = 0.9997$.

$$\mathbf{NaCl(mol/L)} = \mathbf{6} \times \mathbf{10^{-5}}\,|\mathbf{S_{21}}|^3 + \mathbf{8} \times \mathbf{10^{-4}}\,|\mathbf{S_{21}}|^2 + \mathbf{0.0516}\,|\mathbf{S_{21}}| - \mathbf{0.194} \quad (1)$$

In order to test the ability of the developed fitting equation to predict concentrations. An additional three saline solutions with concentrations 0.05, 0.35, and 0.7 mol/L corresponding to 2.92, 20.45, and 40.9 g/L were prepared and measured. The given new concentrations have not been used in the model creation. These three solutions were tested with the proposed sensor. The corresponding measured transmission levels were −4.6, −10.9, and −16.2 dB respectively. Equation (1) predicted the concentrations as 0.0323, 0.351, and 0.687 mol/L which corresponds to an absolute error of 0.0177, 0.001, and 0.013 mol/L and a relative error of 35.4, 0.29, and 1.8% respectively. The significant relative error in the 0.05 mol/L concentration prediction may be due to insufficient samples in the 0.01-0.1 mol/L range which consisted of 2 points per decade only whereas the 0.1-1 mol/L range consisted of 4 points per decade. Thus, the curve may be under sampled in this region. Fig 12. shows the fitting function relative to the original measurements and the test samples.

The proposed sensor is capable of distinguishing the sodium chloride concentrations in the range 0.01-0.1 mol/L. This includes the threshold for cystic fibrosis diagnosis (0.06 mol/L). At 2 GHz, S_{21} changes from −3.925 dB for 0.01 mol/L to −4.6 dB at 0.05 mol/L and −5.95 dB at 0.1 mol/L. Thus, the proposed sensor can be used in the diagnosis of CF.

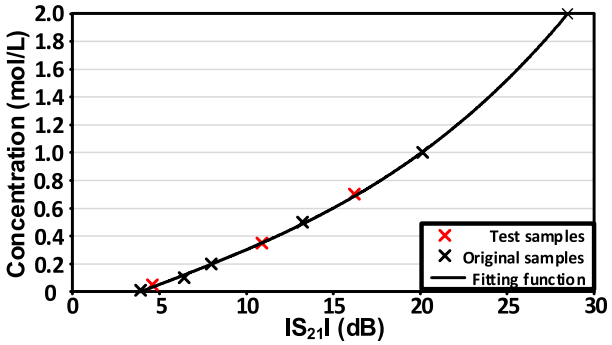

FIGURE 12. Fitted curve for Concentration of LUT (mol/L) versus magnitude of transmission S_{21} in dB using Eq. (1) at 2 GHz. Original measurements are in black and Test samples are in red.

The proposed sensor relies on sampling liquids/sweat with paper superstrate with an overall size of 40 mm × 18 mm. The paper has overall thickness of 180 μm which is highly conformal to sample sweat at any position on human body. One round of measurement involves processing 1001 points with detection time less than 2 minutes. With the proposed sensor, detection decision does not include any conditioning phases or additional circuits. For testing biofluids, the proposed approach is not influenced by contact with the skin or tissues and does not require proximity to the human body for a sensing decision. The proposed sensor acquires broadband spectrum as transmission-based systems. This allows characterization of liquid under test at different frequencies in single measurement round. Compared to the work in [23], the microwave circuit is fixed and only the paper superstrate is disposed with each new LUT. This can reduce the overall cost of sensing system to the price of the paper itself around 5-10 cents. This price point place the proposed sensor in reusable category which is highly appealing in clinical practices and daily monitoring.

VII. CONCLUSION

This work proposed a low-cost, re-usable microwave-based liquid sensor in the band of 1-6 GHz. The proposed sensor could be used to monitor hydration status and to diagnose cystic fibrosis through tracking concentration of NaCl in sweat. The sensor was able to detect concentrations of NaCl as low as 0.01 mol/L with quantities as low as 137 μL. The sensor had a maximum sensitivity of 6.716 dB/g/L at 2 GHz and 46.7 dB/g/L at 6 GHz with dynamic range of 2 mol/L. Using models of artificial sweat, the sensor was able to distinguish between normal and dehydrated states. Compared to other sensors presented in literature, the proposed sensor has a simpler structure, simpler sampling mechanism for liquids, excelling performance, enhanced sensitivity as well as lower operating costs. The proposed sensor is not limited to sweat monitoring but could also fit in several agriculture and industrial applications that require fast response liquid characterization.

ACKNOWLEDGMENT

The authors would like to thank Dr. A. Mohsen in Chemistry lab, Faculty of engineering, Ain Shams university in Cairo,

EGYPT for providing access to their facilities. They also like to thank Prof. E. Fear at Schulich School of Engineering at University of Calgary, CANADA for providing us with the filter paper used in the experimental procedures.

REFERENCES

[1] Accessed: Jun. 20, 2020. [Online]. Available: https://www.who.int/genomics/public/geneticdiseases/en/index2.html#CF

[2] Accessed: Jun. 20, 2020. [Online]. Available: https://www.cfww.org/what-is-cystic-fibrosis

[3] P. M. Farrell, "Diagnosis of Cystic Fibrosis: Consensus Guidelines from the Cystic Fibrosis Foundation," *The J. Pediatrics*, vol. 181, pp. 1–15, Feb. 2017. [Online]. Available: https://www.cff.org/Care/Clinical-Care-Guidelines/Diagnosis-Clinical-Care-Guidelines/Sweat-Test-Clinical-Care-Guidelines/, doi: 10.1016/j.jpeds.2016.09.064.

[4] Accessed: Jul. 23, 2020. [Online]. Available: https://www.mayoclinic.org/diseases-conditions/dehydration/symptoms-causes/syc-20354086

[5] Accessed: Jun. 20, 2020. [Online]. Available: https://www.cdc.gov/ncbddd/dvt/facts.html

[6] Accessed: Jun. 20, 2020. [Online]. Available: https://www.nhs.uk/conditions/deep-vein-thrombosis-dvt/

[7] Accessed: Jun. 20, 2020. [Online]. Available: https://www.cdc.gov/ncbddd/dvt/infographic-impact.html

[8] National Health Commission of China. Accessed: Jan. 22, 2020. *New Coronavirus Pneumonia Prevention and Control Program*. [Online]. Available: http://www.gov.cn/zhengce/zhengceku/2020-01/28/5472673/files/0f96c10cc09d4d36a6f9a9f0b42d972b.pdf

[9] B. Zhou, J. She, Y. Wang, and X. Ma, "Venous thrombosis and arteriosclerosis obliterans of lower extremities in a very severe patient with 2019 novel coronavirus disease: A case report," *J. Thrombosis Thrombolysis*, vol. 50, no. 1, pp. 229–232, Jul. 2020, doi: 10.1007/s11239-020-02084-w.

[10] S. H. Faulkner, K. L. Spilsbury, J. Harvey, A. Jackson, J. Huang, M. Platt, A. Tok, and M. A. Nimmo, "The detection and measurement of interleukin-6 in venous and capillary blood samples, and in sweat collected at rest and during exercise," *Eur. J. Appl. Physiol.*, vol. 114, no. 6, pp. 1207–1216, Jun. 2014, doi: 10.1007/s00421-014-2851-8.

[11] D. P. Rose, M. E. Ratterman, D. K. Griffin, L. Hou, N. Kelley-Loughnane, R. R. Naik, J. A. Hagen, I. Papautsky, and J. C. Heikenfeld, "Adhesive RFID sensor patch for monitoring of sweat electrolytes," *IEEE Trans. Biomed. Eng.*, vol. 62, no. 6, pp. 1457–1465, Jun. 2015, doi: 10.1109/TBME.2014.2369991.

[12] K. De Guzman and A. Morrin, "Screen-printed tattoo sensor towards the non-invasive assessment of the skin barrier," *Electroanalysis*, vol. 29, no. 1, pp. 188–196, Jan. 2017, doi: 10.1002/elan.201600572.

[13] W. Gao, S. Emaminejad, H. Y. Y. Nyein, S. Challa, K. Chen, A. Peck, H. M. Fahad, H. Ota, H. Shiraki, D. Kiriya, D.-H. Lien, G. A. Brooks, R. W. Davis, and A. Javey, "Fully integrated wearable sensor arrays for multiplexed *in situ* perspiration analysis," *Nature*, vol. 529, no. 7587, pp. 509–514, Jan. 2016, doi: 10.1038/nature16521.

[14] P. Velez, K. Grenier, J. Mata-Contreras, D. Dubuc, and F. Martin, "Highly-sensitive microwave sensors based on open complementary split ring resonators (OCSRRs) for dielectric characterization and solute concentration measurement in liquids," *IEEE Access*, vol. 6, pp. 48324–48338, 2018, doi: 10.1109/ACCESS.2018.2867077.

[15] A. Babajanyan, J. Kim, S. Kim, K. Lee, and B. Friedman, "Sodium chloride sensing by using a near-field microwave microprobe," *Appl. Phys. Lett.*, vol. 89, no. 18, p. 151, Oct. 2006, Art. no. 183504, doi: 10.1063/1.2374681.

[16] A. Bababjanyan, H. Melikyan, S. Kim, J. Kim, K. Lee, and B. Friedman, "Real-time noninvasive measurement of glucose concentration using a microwave biosensor," *J. Sensors*, vol. 2010, Dec. 2010, Art. no. 452163, doi: 10.1155/2010/452163.

[17] S. Kim, H. Melikyan, J. Kim, A. Babajanyan, J.-H. Lee, L. Enkhtur, B. Friedman, and K. Lee, "Noninvasive *in vitro* measurement of pig-blood d-glucose by using a microwave cavity sensor," *Diabetes Res. Clin. Pract.*, vol. 96, no. 3, pp. 379–384, Jun. 2012, doi: 10.1016/j.diabres.2012.01.018.

[18] N. Sharafadinzadeh, M. Abdolrazzaghi, and M. Daneshmand, "Highly sensitive microwave split ring resonator sensor using gap extension for glucose sensing," in *IEEE MTT-S Int. Microw. Symp. Dig.*, Pavia, Lombardy, Sep. 2017, pp. 1–3, doi: 10.1109/IMWS-AMP.2017.8247400.

[19] J. Kim, A. Babajanyan, A. Hovsepyan, K. Lee, and B. Friedman, "Microwave dielectric resonator biosensor for aqueous glucose solution," *Rev. Sci. Instrum.*, vol. 79, no. 8, Aug. 2008, Art. no. 086107, doi: 10.1063/1.2968115.

[20] L. Odabashyan, A. Babajanyan, Z. Baghdasaryan, S. Kim, J. Kim, B. Friedman, J.-H. Lee, and K. Lee, "Real-time noninvasive measurement of glucose concentration using a modified Hilbert shaped microwave sensor," *Sensors*, vol. 19, no. 24, p. 5525, Dec. 2019, doi: 10.3390/s19245525.

[21] P. Velez, J. Mata-Contreras, D. Dubuc, K. Grenier, and F. Martin, "Solute concentration measurements in diluted solutions by means of split ring resonators," in *Proc. 48th Eur. Microw. Conf. (EuMC)*, Madrid, India, Sep. 2018, pp. 231–234, doi: 10.23919/EuMC.2018.8541523.

[22] P. Vélez, J. Muñoz-Enano, K. Grenier, J. Mata-Contreras, D. Dubuc, and F. Martín, "Split ring resonator-based microwave fluidic sensors for electrolyte concentration measurements," *IEEE Sensors J.*, vol. 19, no. 7, pp. 2562–2569, Apr. 2019, doi: 10.1109/JSEN.2018.2890089.

[23] A. Eldamak and E. Fear, "Conformal and disposable antenna-based sensor for non-invasive sweat monitoring," *Sensors*, vol. 18, no. 12, p. 4088, Nov. 2018, doi: 10.3390/s18124088.

[24] A. R. Eldamak, S. Thorson, and E. C. Fear, "Study of the dielectric properties of artificial sweat mixtures at microwave frequencies," *Biosensors*, vol. 10, no. 6, p. 62, Jun. 2020, doi: 10.3390/bios10060062.

[25] J. Moyer, D. Wilson, I. Finkelshtein, B. Wong, and R. Potts, "Correlation between sweat glucose and blood glucose in subjects with diabetes," *Diabetes Technol. Therapeutics*, vol. 14, no. 5, pp. 398–402, May 2012, doi: 10.1089/dia.2011.0262.

[26] K. Sakaguchi, Y. Hirota, N. Hashimoto, W. Ogawa, T. Hamaguchi, T. Matsuo, J.-I. Miyagawa, M. Namba, T. Sato, S. Okada, K. Tomita, M. Matsuhisa, H. Kaneto, K. Kosugi, H. Maegawa, H. Nakajima, and A. Kashiwagi, "Evaluation of a minimally invasive system for measuring glucose area under the curve during oral glucose tolerance tests: Usefulness of sweat monitoring for precise measurement," *J. Diabetes Sci. Technol.*, vol. 7, no. 3, pp. 678–688, May 2013, doi: 10.1177/193229681300700313.

[27] D. C. Garrett, N. Rae, J. R. Fletcher, S. Zarnke, S. Thorson, D. B. Hogan, and E. C. Fear, "Engineering approaches to assessing hydration status," *IEEE Rev. Biomed. Eng.*, vol. 11, no. 5, pp. 233–248, Oct. 2018, doi: 10.1109/RBME.2017.2776041.

[28] W. Dawsmith, N. Ohtani, R. Donnan, M. Naftaly, R. A. Dudley, and T. T. Chowdhury, "Microwave frequency dependent dielectric properties of blood as a potential technique to measure hydration," *IEEE Access*, early access, 2020, doi: 10.1109/ACCESS.2020.2977432.

[29] L. A. Bronckers, M. J. R. A. van Rossum, and A. B. Smolders, "Planar sensors for dielectric and magnetic materials measurement: A quantitative sensitivity comparison," in *Proc. 12th Eur. Conf. Antennas Propag. (EuCAP)*, 2018, pp. 1–4, doi: 10.1049/cp.2018.0650.

[30] C.-H. Chio, C. Teng, K.-W. Tam, W.-W. Choi, P. Cheong, and S.-K. Ho, "Differential permittivity sensor using microstrip terminated cross-shaped resonator structure for material characterization," *IEEE Access*, vol. 7, pp. 101960–101968, 2019, doi: 10.1109/ACCESS.2019.2930747.

[31] A. A. M. Bahar, Z. Zakaria, S. R. Ab Rashid, A. A. M. Isa, E. Ruslan, and R. A. Alahnomi, "Microstrip planar resonator sensors for accurate dielectric measurement of microfluidic solutions," in *Proc. 3rd Int. Conf. Electron. Des. (ICED)*, Aug. 2016, pp. 416–421, doi: 10.1109/ICED.2016.7804680.

[32] M. A. H. Ansari, A. K. Jha, Z. Akhter, and M. J. Akhtar, "Multi-band RF planar sensor using complementary split ring resonator for testing of dielectric materials," *IEEE Sensors J.*, vol. 18, no. 16, pp. 6596–6606, 15 Aug. 15, 2018, doi: 10.1109/JSEN.2018.2822877.

[33] O. J. Babarinde, A. Petrocchi, V. Volskiy, I. Ocket, and D. Schreurs, "Development of a planar microwave resonator based wetness sensor," in *Proc. 11th German Microw. Conf. (GeMiC)*, Freiburg, Germany, Mar. 2018, pp. 199–202, doi: 10.23919/GEMIC.2018.8335064.

[34] M. Shafi, A. K. Jha, and M. J. Akhtar, "Nondestructive technique for detection of adulteration in edible oils using planar RF sensor," in *IEEE MTT-S Int. Microw. Symp. Dig.*, New Delhi, India, Dec. 2016, pp. 1–4, doi: 10.1109/IMaRC.2016.7939636.

[35] A. K. Jha, Z. Akhter, N. Tiwari, K. T. M. Shafi, H. Samant, M. J. Akhtar, and M. Cifra, "Broadband wireless sensing system for non-invasive testing of biological samples," *IEEE J. Emerg. Sel. Topics Circuits Syst.*, vol. 8, no. 2, pp. 251–259, Jun. 2018, doi: 10.1109/JETCAS.2018.2829205.

[36] N. K. Tiwari, S. P. Singh, and M. J. Akhtar, "Coplanar waveguide based planar RF sensor for the detection of adulteration in oils," in *Proc. IEEE Appl. Electromagn. Conf. (AEMC)*, Aurangabad, Germany, 2017, pp. 1–2, doi: 10.1109/AEMC.2017.8325754.

[37] W. Liu, M. Wang, and Y. Shi, "A transmission-reflection method for complex permittivity measurement using a planar sensor," *IEEE Sensors J.*, vol. 18, no. 10, pp. 4059–4065, May 2018, doi: 10.1109/JSEN.2018.2820079.
[38] M. Abdolrazzaghi, M. H. Zarifi, W. Pedrycz, and M. Daneshmand, "Robust ultra-high resolution microwave planar sensor using fuzzy neural network approach," *IEEE Sensors J.*, vol. 17, no. 2, pp. 323–332, Jan. 2017, doi: 10.1109/JSEN.2016.2631618.
[39] A. A. M. Bahar, Z. Zakaria, S. R. Ab Rashid, A. A. M. Isa, R. A. Alahnomi, and Y. Dasril, "Microfluidic planar resonator sensor with highly precise measurement for microwave applications," in *Proc. 11th Eur. Conf. Antennas Propag. (EUCAP)*, Mar. 2017, pp. 1843–1846, doi: 10.23919/EuCAP.2017.7928521.
[40] A. M. Albishi and O. M. Ramahi, "Highly sensitive microwaves sensors for fluid concentration measurements," *IEEE Microw. Wireless Compon. Lett.*, vol. 28, no. 4, pp. 287–289, Apr. 2018, doi: 10.1109/LMWC.2018.2805866.
[41] M. Abdolrazzaghi, M. Daneshmand, and A. K. Iyer, "Strongly enhanced sensitivity in planar microwave sensors based on metamaterial coupling," *IEEE Trans. Microw. Theory Techn.*, vol. 66, no. 4, pp. 1843–1855, Apr. 2018, doi: 10.1109/TMTT.2018.2791942.
[42] A. Stogryn, "Equations for calculating the dielectric constant of saline water (Correspondence)," *IEEE Trans. Microw. Theory Techn.*, vol. 19, no. 8, pp. 733–736, Aug. 1971, doi: 10.1109/TMTT.1971.1127617.
[43] M. Said, M. Amr, Y. Sabry, D. Khalil, and A. Wahba, "Plastic sorting based on MEMS FTIR spectral chemometrics sensing," *Proc. SPIE Opt. Sens. Detection*, vol. 11354, May 2020, Art. no. 113540J, doi: 10.1117/12.2555876.
[44] M. Amr, Y. M. Sabry, and D. Khalil, "Near-infrared optical MEMS spectrometer-based quantification of fat concentration in milk," in *Proc. 35th Nat. Radio Sci. Conf. (NRSC)*, Mar. 2018, pp. 409–416, doi: 10.1109/NRSC.2018.8354389.
[45] M. M. Y. R. Riad, Y. M. Sabry, and D. Khalil, "On the detection of volatile organic compounds (VOCs) using machine learning and FTIR spectroscopy for air quality monitoring," in *Proc. 36th Nat. Radio Sci. Conf. (NRSC)*, Apr. 2019, pp. 386–392, doi: 10.1109/NRSC.2019.8734644.

MICHAEL M. Y. R. RIAD was born in Cairo, Egypt, in 1994. He received the B.Sc. degree (Hons.) in electrical engineering from Ain Shams University, Cairo, in 2018, where he is currently pursuing the M.Sc. degree. From 2018 to 2020, he was working part-time as a Teaching/Research Assistant with the Faculty of Engineering, Ain Shams University. From 2019 to 2020, he was working with Mentor, A Siemens Business. In 2020, He became a full-time Teaching/Research Assistant with the Faculty of Engineering, Ain Shams University. His research interests include microwave sensors, FTIR spectroscopy, and machine learning.

A. R. ELDAMAK (Member, IEEE) was born in Damietta, Egypt, in 1980. She received the B.Sc. and M.Sc. degrees in electrical engineering from Ain Shams University, Cairo, Egypt, in 2002 and 2006, respectively, and the Ph.D. degree in electrical engineering from Ryerson University, Toronto, Canada, in 2013. Since November 2014, she has been with the Electronics and Communications Engineering Department, Ain Shams University, where she is an Assistant Professor. Her current research interests include antennas, microwave-based sensors, and passive microwave components. She has 12 years of microwave R&D experience specifically in designing passive antenna systems as well as fabrication and testing for bio-sensing and wireless communications applications, eight years of R&D experience in designing, implementing, and modeling fiber-based systems.